

# Mechanistic Investigation of the Dipolar [2 + 2] Cycloaddition–Cycloreversion Reaction between 4-(*N,N*-Dimethylamino)phenylacetylene and Arylated 1,1-Dicyanovinyl Derivatives To Form Intramolecular Charge-Transfer Chromophores

Yi-Lin Wu, Peter D. Jarowski, W. Bernd Schweizer, and François Diederich\*<sup>[a]</sup>

**Abstract:** The kinetics and mechanism of the formal [2+2] cycloaddition–cycloreversion reaction between 4-(*N,N*-dimethylamino)phenylacetylene (**1**) and *para*-substituted benzylidenemalononitriles **2b–2l** to form 2-donor-substituted 1,1-dicyanobuta-1,3-dienes **3b–3l** via the postulated dicyanocyclobutene intermediates **4b–4l** have been studied experimentally by the method of initial rates and computationally at the unrestricted B3LYP/6-31G(d) level. The transformations were found to follow bimolecular, second-order kinetics, with  $\Delta H_{\text{exp}}^{\ddagger} = 13\text{--}18 \text{ kcal mol}^{-1}$ ,  $\Delta S_{\text{exp}}^{\ddagger} \approx -30 \text{ cal K}^{-1} \text{ mol}^{-1}$ , and  $\Delta G_{\text{exp}}^{\ddagger} = 22\text{--}27 \text{ kcal mol}^{-1}$ . These experimental activation parameters for the rate-de-

termining cycloaddition step are close to the computational values. The rate constants show a good linear free energy relationship ( $\rho = 2.0$ ) with the electronic character of the *para*-substituents on the benzylidene moiety in dimethylformamide (DMF), which is indicative of a dipolar mechanism. Analysis of the computed structures and their corresponding solvation energies in acetonitrile suggests that the rate-determining attack of the nucleo-

philic, terminal alkyne carbon onto the dicyanovinyl electrophile generates a transient zwitterion intermediate with the negative charge developing as a stabilized malononitrile carbanion. The computational analysis predicted that the cycloreversion of the postulated dicyanocyclobutene intermediate would become rate-determining for 1,1-dicyanoethene (**2m**) as the electrophile. The dicyanocyclobutene **4m** could indeed be isolated as the key intermediate from the reaction between alkyne **1** and **2m** and characterized by X-ray analysis. Facile first-order cycloreversion occurred upon further heating, yielding as the sole product the 1,1-dicyanobuta-1,3-diene **3m**.

**Keywords:** cycloaddition • kinetics • linear free energy relationships • push–pull chromophores • reaction mechanisms

## Introduction

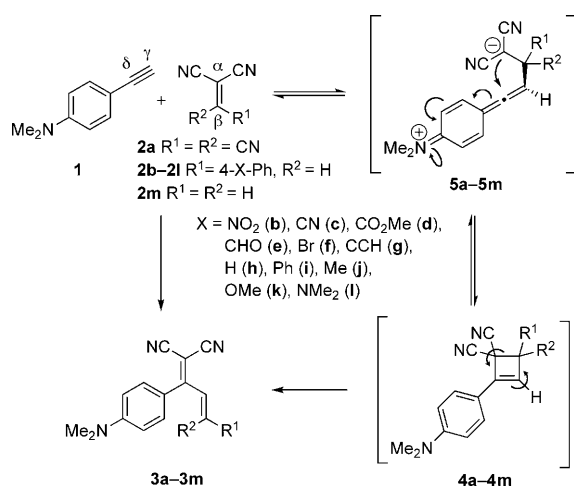
$\pi$ -Conjugated organic donor–acceptor (D- $\pi$ -A) chromophores, featuring intense low-energy intramolecular charge-transfer (CT) absorptions in the visible to near-IR (infrared) spectroscopic range, are in high demand for applications in photonics and nonlinear optics.<sup>[1]</sup> Versatile organic synthesis makes these dipolar organic push–pull molecules highly at-

tractive for fine-tuning their optoelectronic properties and ultimately tailoring and optimizing advanced materials.

Organic D- $\pi$ -A molecules not only need to feature desirable molecular properties but they should also be preparable on a larger scale through fast and efficient transformations. With this in mind, we developed over the last few years ‘click-chemistry’-type<sup>[2]</sup> reactions, which yielded new families of intramolecular CT chromophores. [2+2] Cycloadditions between electron-rich alkynes, such as 4-ethynyl-*N,N*-dimethylaniline (**1**, Scheme 1), and strongly electron-accepting olefins, such as tetracyanoethene (TCNE, **2a**) or 7,7,8,8-tetracyanoquinodimethane (TCNQ), followed by cycloreversion provided nonplanar, donor-substituted 1,1,4,4-tetracyanobuta-1,3-dienes (TCBDs, such as **3a**) and expanded TCNQ derivatives, featuring readily tuneable CT absorption wavelengths, large nonlinear optical responses, and high electron affinities.<sup>[3]</sup> These transformations are generally fast, high-yielding, catalyst-free, 100% atom-economic, and

[a] Y.-L. Wu, Dr. P. D. Jarowski, Dr. W. B. Schweizer, Prof. Dr. F. Diederich  
Laboratorium für Organische Chemie  
ETH-Zürich  
Hönggerberg, HCI  
CH-8093 Zürich (Switzerland)  
Fax: (+41) 44 632 1109  
E-mail: [diederich@org.chem.ethz.ch](mailto:diederich@org.chem.ethz.ch)

Supporting information for this article is available on the WWW under <http://dx.doi.org/10.1002/chem.200902645>.



Scheme 1. The proposed reaction mechanism for the [2+2] cycloaddition–cycloreversion between **1** and cyanoolefins **2** through the zwitterionic (**5**) and cyclobutenyl (**4**) intermediates to form charge-transfer chromophores **3** where X is varied as defined (**b–l**).

the resulting products can be easily purified by precipitation or washing. Recently, a high-speed optical waveguide was prepared from a donor-substituted TCBD.<sup>[4]</sup> The success of these molecules in the materials application arena stems from their ability to form amorphous films of excellent optical quality due to their molecular nonplanarity and sublimability.

More recently, we serendipitously discovered that 1,1-dicyanovinyl derivatives are sufficiently electron-accepting to react with electron-rich alkynes in the same manner as TCNE or TCNQ, providing the nonplanar push–pull chromophores **3** in high yield (Scheme 1).<sup>[5]</sup> A series of *para*-substituted benzylidenemalononitriles (containing many of the compounds in the series **2b–2l**) was successfully converted and the ease of reaction directly correlated with the electron-accepting power of the attached *para*-substituent.

The apparent net reaction for electrophiles **2a–2m** is identical to the transition-metal-catalyzed/mediated enyne metathesis reaction<sup>[6]</sup> both of which provide buta-1,3-diene products. By analogy, we have proposed that the reaction between electron-rich acetylenes and cyanoolefins proceeds through the cyclobutene intermediate **4**. Subsequent cycloreversion (**4**→**3**) of this transient intermediate gives the final cyanobutadienes. Moreover, based on the facts that i) the direct and concerted [2+2] cycloaddition is thermally symmetry-forbidden, ii) the transformation occurs in the absence of a transition-metal catalyst, and iii) the reaction only proceeds between highly polarized components, we further proposed a stepwise, zwitterionic pathway whereby initial nucleophilic addition of the electron-rich alkyne forms a transient zwitterion (**5**) that quickly cyclizes to the cyclobutene. However, except for some information gained by our initial computational investigation<sup>[5]</sup> of the reaction between **1** and 1,1-dicyanoethene (**2m**), TCNE (**2a**), and tricyanoethene (TCE) as electrophiles, little is known about the energetics and relative importance of these intermediates, and

the transition states (TSs), which connect them, towards the overall efficiency and outcome of this versatile class of chemical transformations. Computation suggested that the reaction should be bimolecular in both reactants with a single rate-determining step (RDS). The rate-determining TS, the addition of the alkyne to the electrophile in the case of TCNE and TCE, is strongly polarized according to natural bond orbital (NBO) analysis and is apparent by inspection of the optimized geometries. Additionally, the solvation energies in acetonitrile of the TS for **1**+**2m** and its immediate product **4m** are quite large suggesting strong polarization (the addition step is not rate-determining in this case but rather the ring-opening step, as discussed below). However, there is no direct experimental evidence that proves this zwitterionic mechanism or indicates any of the intermediates. Additionally, there is no evidence that could rule out a thermally allowed diradical mechanism. The question remains to what extent the reactions proceed via zwitterionic or diradical intermediates.

Similar stepwise, zwitterionic mechanisms of pericyclic reactions are known and are especially efficient when highly polarized, nucleophilic and electrophilic unsaturated reactants are involved; many examples of cyclobutane formation through zwitterionic intermediates can be found in classic reviews by Gompper, Huisgen, and Fatiadi.<sup>[7a–d]</sup> However, compared to the reactions between two olefins,<sup>[7]</sup> far less attention has been paid to the triple bond in such dipolar, formal [2+2] cycloadditions.<sup>[8]</sup> Previous studies on the triple bond employed the strongly activated ynamines as the nucleophilic reactants.<sup>[9]</sup> In some cases, cyclobutenes have even been isolated as final products but the relationship between these cycles and the starting materials has been obscured by rearrangements of the peripheral substituents. In other cases, an enyne metathesis happened to give butadienes, but without detection or isolation of the cyclic intermediate. Thus, no mechanistic elucidation has been possible due to the complexity of the chemistry and the lack of a systematic approach to study the electronic and structural aspects of this transformation.

Herein, we present a thorough mechanistic investigation of the [2+2] cycloaddition–cycloreversion reaction between electron-rich alkynes, such as **1**, and electron-deficient dicyanoolefins, such as **2b–2m**, based on both experimental and computational methods. We provide strong evidence for the zwitterionic character of the cycloaddition step and, in one case, report the isolation and characterization of the dicyanocyclobutene intermediate, which is converted to the 1,1-dicyanobuta-1,3-diene as the sole product.

## Results and Discussion

**Order of the reaction and the rate law:** To gain more information about the course of the reaction, a real-time NMR study was performed for the transformation of the benzylidenemalononitriles **2b–2l** in the temperature range from 298 K to 373 K. For a typical example, the <sup>1</sup>H NMR spectral

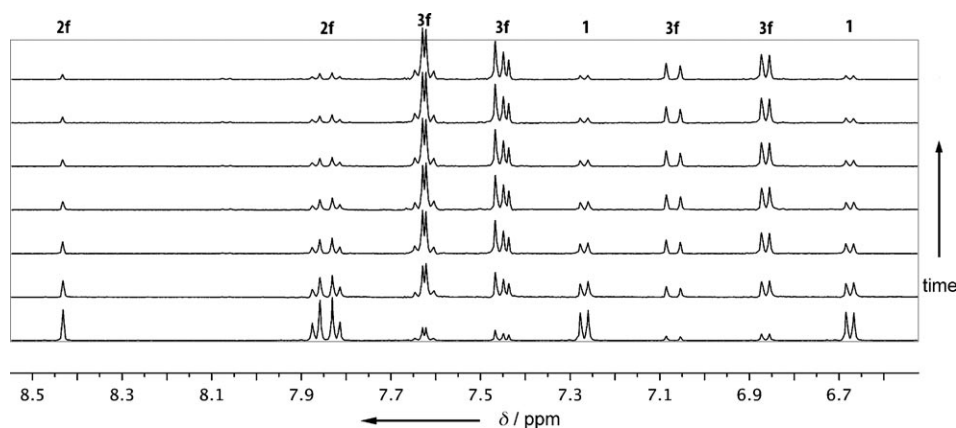


Figure 1. Partial time-dependent  $^1\text{H}$  NMR spectra (500 MHz,  $(\text{CD}_3)_2\text{SO}$ , 373 K) of the solution of **1** and **2f**. The time interval between consecutive traces is 800 s. Structure-signal assignments are given.

evolution of the solution of a 1:1 mixture of **1** and **2f** ( $\text{R}^1 = 4\text{-PhBr}$ ,  $\text{R}^2 = \text{H}$ ) in  $(\text{CD}_3)_2\text{SO}$  at 373 K is shown in Figure 1. Similar spectral changes were observed for all the other *para*-substituted substrates. In all cases, the transformation is clean, directly from starting material to the corresponding *s-trans*, *trans* butadiene product, without any evidence of side-product or transient species formation on the NMR time-scale.

The lack of a pre-equilibrium and the absence of any intermediate structure support our previous computational studies, which predicted a bimolecular reaction mechanism with one key RDS. It is reasonable to rule out any reversibility after the RDS based on the high yields and the rapidity of the reaction under study. Moreover, when the extent of the reaction from NMR data was plotted against the reaction time, simple evolution curves were observed. Under the conditions where the initial concentrations of **1** and **2** are

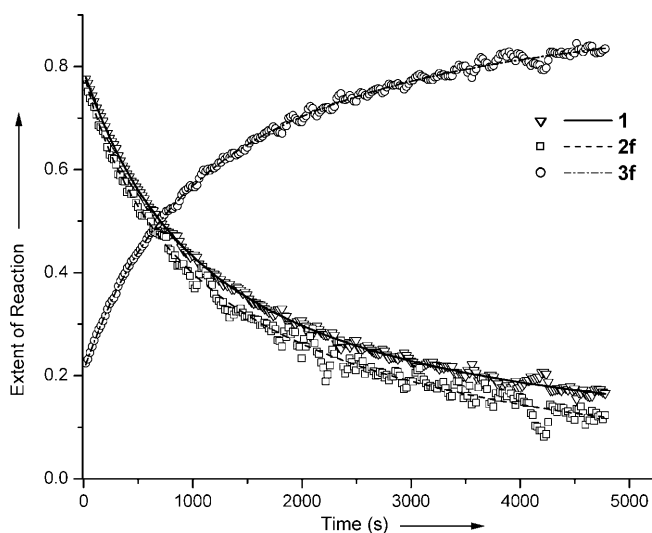


Figure 2. Time evolution of the reaction between **1** and **2f** to give **3f**. The extent of reaction for the reactants is defined as the ratio between the number of one species at time  $t$  to its initial number ( $t=0$ ); for the product, it is defined as the ratio between its number at time  $t$  to the initial number of the reactant.

identical, that is,  $[\mathbf{1}]_0 = [\mathbf{2}]_0$ , the plot fits well to an overall second-order rate expression, meaning first-order in both **1** and **2** throughout the whole course of reaction (Figure 2; for plot-fitting, see the Supporting Information). This was further confirmed by following the evolution of the CT band in the UV/Vis spectrum (see the Supporting Information). The rate of reaction of **2h** ( $\text{R}^1 = \text{Ph}$ ,  $\text{R}^2 = \text{H}$ ) with **1** was monitored at varying reactant ratios (up to threefold excess of one component), and the

rate of product formation was found to be proportional to either  $[\mathbf{1}]$  or  $[\mathbf{2h}]$ , that is, first order in both reactants. Thus, the apparent rate law of the reaction subclass under question is bimolecular and first order in both reactants, Equation (1),

$$v = k[\mathbf{1}][\mathbf{2}] \quad (1)$$

where  $k$  is the observed rate constant. The simplicity of the rate expression in these cases further allows the employment of initial-rate methods in the following kinetics studies without over-simplifying the reaction mechanism. Thus, the initial rate constants are calculated according to Equation (2),

$$k = \frac{d[\mathbf{3}]}{dt} \frac{1}{[\mathbf{1}]_0[\mathbf{2}]_0} \quad (2)$$

where  $d[\mathbf{3}]/dt$  is the observed rate and  $[\mathbf{1}]_0$  and  $[\mathbf{2}]_0$  are the initial concentrations of **1** and **2**.

**Rate-dependency on the electronic nature of the substituents:** A series of *para*-substituted benzylidenemalononitriles **2b–2k** was mixed with **1** in DMF (*N,N*-dimethylformamide) solution at 298 K, and the development of their characteristic CT bands around 450 nm was used to monitor the rate of product formation and to determine the rate constant by the method of initial rates employing Equation (2) as the kinetic model. As shown in the inset of Figure 3, the intensity of the CT band increases vertically, again suggesting a clean transformation without by-product formation.

The logarithms of the measured initial-rate constants of compounds **2b–2k** with *para*-substituent X relative to the logarithm of the rate of **2h** ( $\text{X} = \text{H}$ ) were plotted against their corresponding Hammett substituent constants  $\sigma_p$ ,<sup>[10]</sup> and a good linear correlation was found ( $R^2 = 0.97$ ), with slope  $\rho = 2.0 \pm 0.1$  (Figure 3). Each data point was measured independently three times and the average rate constant presented in Figure 3. The standard deviations are in the range of 10% in most cases. The plot containing **2l** at 373 K also exhibits a linear free-energy relationship. Data at 323

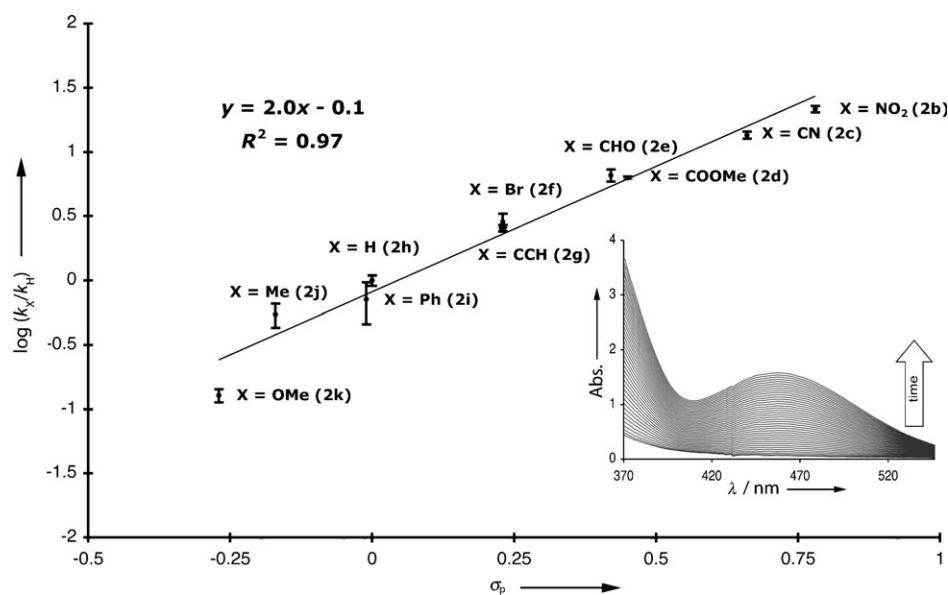


Figure 3. Hammett plot of initial rate constants of the reaction of **1** with electrophiles **2b–2k** relative to the initial rate constant for **2h** versus the Hammett substituent constants  $\sigma_p$  at 298 K. The inset shows the time evolution (in the direction of the arrow) of the CT band for the reaction of **1** with **2h**.

and 348 K including **2b–2k** have also been obtained (see the Supporting Information). As depicted in Figure 3, the good linearity implies that the same reaction mechanism is operating for all derivatives; the moderately positive  $\rho$  value reflects that the reaction is accelerated by electron-withdrawing substituents and signifies a buildup of electron density around the benzylidene ring in the RDS, consistent with a stepwise, zwitterionic mechanism where nucleophilic addition to the 1,1-dicyanovinyl (DCV) moiety pushes electrons to the most stabilizing 1,1-dicyanomethylidene position.

It was not possible to measure the rate of reaction of **1** and **2l** at 298 K due to its sluggishness; the evolution of the CT band was obscured by instrument noise. Kinetic data at 373 K that include this point are presented in the Supporting Information and show a linear correlation.

**Calculated free energy profile by density functional theory and activation parameters by Eyring analysis:** In our previous report, a reaction free-energy profile was examined for the reaction between **1** and methylenemalononitrile (**2m**) at the unrestricted B3LYP/6-

31G(d) level<sup>[11]</sup> in the gas-phase as well as using the polarizable continuum model (PCM) with acetonitrile to model solvent effects. Herein, this methodology is extended to the cases of the reaction of **1** with the electrophiles having *para*-nitrophenyl (**2b**), phenyl (**2h**), or *para*-dimethylanilino (**2l**) moieties attached to the DCV group, treating only the most relevant points along the reaction profile that are candidates for the RDS. The stability of the wavefunction was verified in each case. Geometries were optimized using the program Gaussian 03.<sup>[11]</sup> Stationary points were characterized by harmonic vibrational frequency analysis. Molecular energies were calculated as the

sum of the electronic energy and Gibbs free energy correction obtained from these analytical frequencies at 298.15 K. The Supporting Information gives all necessary numerical values used in this work along with zero-point and thermal corrections, gas-phase and solvated energies and geometries.

Irrespective of the substituent on the electrophile, the reaction consists of four basic steps (Figure 4). From unreact-

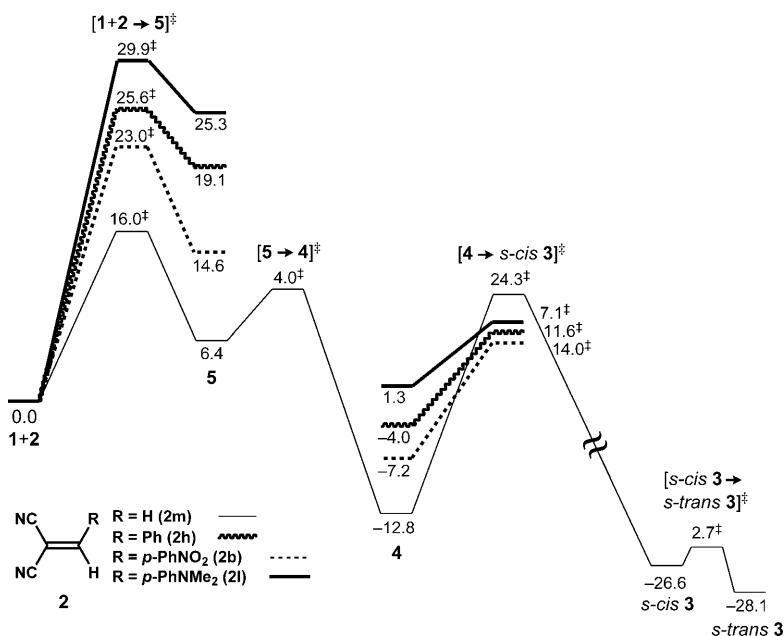


Figure 4. Free-energy reaction profile at the B3LYP/6-31G(d) level (with PCM solvation in acetonitrile) for **2m** (thin solid line), **2b** (dashed line), **2h** (wavy line), and **2l** (thick solid line) with energies (kcal mol<sup>-1</sup>) provided for reactants (**1+2**) (reference energy), intermediates **5**, **4**, *s-cis* **3**, and product *s-trans* **3**, and transition-states barriers [**1+2**→**5**]<sup>‡</sup>, [**5**→**4**]<sup>‡</sup>, [**4**→*s-cis* **3**]<sup>‡</sup> and [*s-cis* **3**→*s-trans* **3**]<sup>‡</sup> (energies referenced to their preceding intermediate).

ed components (**1+2**), nucleophilic addition of the  $\gamma$ -carbon of the terminal alkyne (**1**) to the  $\beta$ -position of the electrophile (**2**) occurs to produce a high-energy intermediate (**5**) through the bond-forming transition state (TS) (**[1+2→5]<sup>‡</sup>**) (see Scheme 1 for notation). From here, the ring-closed product (**4**) is obtained by bond formation between the  $\alpha$  and  $\delta$  carbons through an electrocyclic TS (**[5→4]<sup>‡</sup>**). For the reaction between **1** and **2m**, this happens through a barrier only slightly more energetic compared to the corresponding energy of **5** and slightly less than the energy of **[1+2m→5m]<sup>‡</sup>**, but the analogous TSs could not be located for the reaction with electrophiles **2b**, **2h**, and **2l**, presumably due to their shallow potential energy wells, which precluded optimization to their respective stationary states. Moving forward, the ring-opening cycloreversion step breaks the  $\alpha$ - $\beta$  bond (**[4→s-cis 3]<sup>‡</sup>**) leading eventually to the final products (*s-trans* **3**) by *s-cis*-to-*s-trans* isomerization (**[s-cis 3→s-trans 3]<sup>‡</sup>**).

There is a considerable substituent effect on the TS energetics of the addition step **[1+2→5]<sup>‡</sup>**. In the non-substituted case, 1,1-dicyanoethylene **2m** reacts through a mechanism where the ring-opening process (**[4m→s-cis 3m]<sup>‡</sup>**;  $\Delta G_{\text{calcd}}^{\ddagger} = 24.3 \text{ kcal mol}^{-1}$ ) is rate-determining based on comparison of the calculated free-energies of activation in acetonitrile (compare to **[1+2m→5m]<sup>‡</sup>** in which  $\Delta G_{\text{calcd}}^{\ddagger} = 16.0 \text{ kcal mol}^{-1}$ ), while in the case of the 1,1-dicyanovinylphenylenes **2b**, **2h**, and **2l**, the RDS is the addition step (**[1+2→5]<sup>‡</sup>**;  $\Delta G_{\text{calcd}}^{\ddagger} = 23.0, 25.6, \text{ and } 29.9 \text{ kcal mol}^{-1}$ , respectively; compare to **[4→s-cis 3]<sup>‡</sup>**;  $\Delta G_{\text{calcd}}^{\ddagger} = 14.0, 7.1, \text{ and } 11.6 \text{ kcal mol}^{-1}$ , respectively). Inclusion of a phenyl group at the  $\beta$ -position of the electrophile clearly raises the energy of **[1+2→5]<sup>‡</sup>** in all cases, compared to **2m**, rendering it rate-determining overall. A secondary influence beyond this, presumably steric, effect of the phenyl ring is felt from the electronic nature of the attached substituent at its *para*-position; the nitro-substituted derivative (**2b**) reacts through the lowest barrier, followed by the phenyl group (**2h**) and finally the *N,N*-dimethylamino-substituted reactant (**2l**). Thus, the increased electrophilicity of the dicyanovinyl group caused by electron-withdrawal accelerates the reaction. This is in accordance with the experimental kinetic results.

In contrast, the *para*-phenyl substituent has a diminished influence on the ring-opening TS. The differences in this barrier **[4→s-cis 3]<sup>‡</sup>** for **2b**, **2h**, and **2l** arise mostly from large changes in the energies of the cyclobutene intermediates (**4**). The strongly donating dimethylanilino (DMA) group destabilizes the cycle considerable (**4l**;  $\Delta G_{\text{calcd}} = 1.3 \text{ kcal mol}^{-1}$ ), placing its energy on the endergonic side of the reaction profile compared to this state along the reaction profile of **1+2m** (**4m**;  $\Delta G_{\text{calcd}} = -12.8 \text{ kcal mol}^{-1}$ ). Both *para*-nitrophenyl (**4b**;  $\Delta G_{\text{calcd}} = -7.2 \text{ kcal mol}^{-1}$ ) and phenyl (**4h**;  $\Delta G_{\text{calcd}} = -4.0 \text{ kcal mol}^{-1}$ ) substitution also destabilize the cyclobutene, but to a lesser extent than for **4l**. It is important to notice that the electronic effects of the phenyl substituent on the barriers **[1+2→5]<sup>‡</sup>** and **[4→s-cis 3]<sup>‡</sup>** are exactly opposite to each other. While **[1+2→5]<sup>‡</sup>** lowers upon increased electron-withdrawing character of the sub-

stituent, **[4→s-cis 3]<sup>‡</sup>** raises (due mostly to effects in **4**). Thus, the kinetic results from the Hammett plot (positive  $\rho$  value) are consistent with **[1+2→5]<sup>‡</sup>** as the RDS and rule-out any mechanism with **[4→s-cis 3]<sup>‡</sup>** as the RDS since the sign of  $\rho$  would be reversed to what is experimentally observed.

Solvation energies in acetonitrile for **[1+2→5]<sup>‡</sup>** occur at a relatively constant value ( $\Delta\Delta G_{\text{solvation}}^{\ddagger} = \Delta G_{\text{MeCN,calcd}}^{\ddagger} - \Delta G_{\text{gas,calcd}}^{\ddagger} \approx -3 \text{ kcal mol}^{-1}$ ) and increase significantly for the immediate product **5** ( $\Delta\Delta G_{\text{solvation}} = \Delta G_{\text{MeCN,calcd}} - \Delta G_{\text{gas,calcd}} = -9.5$  (**5m**),  $-10.9$  (**5b**),  $-8.6$  (**5h**) and  $-7.9$  (**5l**)  $\text{kcal mol}^{-1}$ ) (negative values indicate stabilization). Thus, the zwitterionic character of the TS is corroborated, and to a greater extent, this character is prevalent in the intermediate (**5**) with the amount of stabilization increasing with the withdrawing power of the substituent. Solvation energies for **[4→s-cis 3]<sup>‡</sup>** are positive and near  $1 \text{ kcal mol}^{-1}$  in all cases. Somewhat larger numbers are found for the cyclobutenes (**4**), which are destabilized (positive  $\Delta\Delta G_{\text{solvation}}$ ) by  $3.5$ – $4.5 \text{ kcal mol}^{-1}$ . Based on the small and positive solvation energies of **[4→s-cis 3]<sup>‡</sup>**, the zwitterionic character of the ring-opening step should be small. Thus, a concerted diradical mechanism is most likely.

From variable-temperature UV/Vis kinetic data, it was possible to perform Eyring analysis and extract the experimental activation parameters  $\Delta H_{\text{exp}}^{\ddagger}$ ,  $\Delta S_{\text{exp}}^{\ddagger}$ , and  $\Delta G_{\text{exp}}^{\ddagger}$ . The initial rates for the reaction of **1** with electrophiles **2b**, **2h**, and **2l** were monitored in DMF at three or four temperatures and the data fitted to the Eyring expression (for a detailed description, see the Experimental; for the fitting analysis of the Eyring plots, see the Supporting Information). There is excellent quantitative agreement, in addition to the qualitative agreement, between the experimental activation parameters ( $\Delta G_{\text{exp}}^{\ddagger}$  in DMF) obtained from Eyring analysis and the computed values (PCM solvation in acetonitrile) as shown in Table 1.

Table 1. Experimental (298 K, DMF) and calculated (298 K, PCM solvation in MeCN) activation parameters for the cycloaddition reaction between **1** and **2b**, **2g**, and **2l**, and for the ring-opening reaction of **4m**.

Reactants	$\Delta G_{\text{exp}}^{\ddagger}$ [kcal mol <sup>-1</sup> ]	$\Delta G_{\text{calcd}}^{\ddagger}$ [kcal mol <sup>-1</sup> ]	$\Delta H_{\text{exp}}^{\ddagger}$ [kcal mol <sup>-1</sup> ]	$\Delta H_{\text{calcd}}^{\ddagger}$ [kcal mol <sup>-1</sup> ]	$\Delta S_{\text{exp}}^{\ddagger}$ [cal K <sup>-1</sup> mol <sup>-1</sup> ]	$\Delta S_{\text{calcd}}^{\ddagger}$ [cal K <sup>-1</sup> mol <sup>-1</sup> ]
<b>1+2b</b>	22 ± 1	23.0	13 ± 1	11.0	-30.3 ± 0.4	-40.2
<b>1+2h</b>	23.6 ± 0.6	25.6	14.7 ± 0.6	13.8	-29.9 ± 0.2	-39.7
<b>1+2l</b>	27 ± 3	29.9	18 ± 3	18.2	-29.1 ± 0.8	-39.3
<b>4m</b>	27 ± 1	24.3	24 ± 1	23.8	-11.4 ± 0.3	-1.6

The measured activation parameters for **1+2→3** agree with the calculated values for the TS **[1+2→5]<sup>‡</sup>**. The measured negative entropies of activations ( $\approx -30 \text{ cal K}^{-1} \text{ mol}^{-1}$ ) support a mechanism involving a bimolecular RDS. The activation parameters measured for the conversion of **4m**→**3m** (see next section for more details) also agree well with the computed transition-state energy barrier of **[4m→s-cis 3m]<sup>‡</sup>**, and the entropy of activation ( $\Delta S_{\text{exp}}^{\ddagger} = -11.4 \pm 0.3 \text{ cal mol}^{-1} \text{ K}^{-1}$ ) is consistent with a unimolecular RDS pro-

cess. The experimental free energies of activation agree with those computed to an average absolute deviation of 2 kcal mol<sup>-1</sup>. While this is not proof that the RDS has been unambiguously assigned, it lends credence to the computational approach and methodology presented here.

The geometric parameters strongly suggest zwitterionic character in the addition TS ([1+2→5]<sup>‡</sup>) for all derivatives (Figure 5).

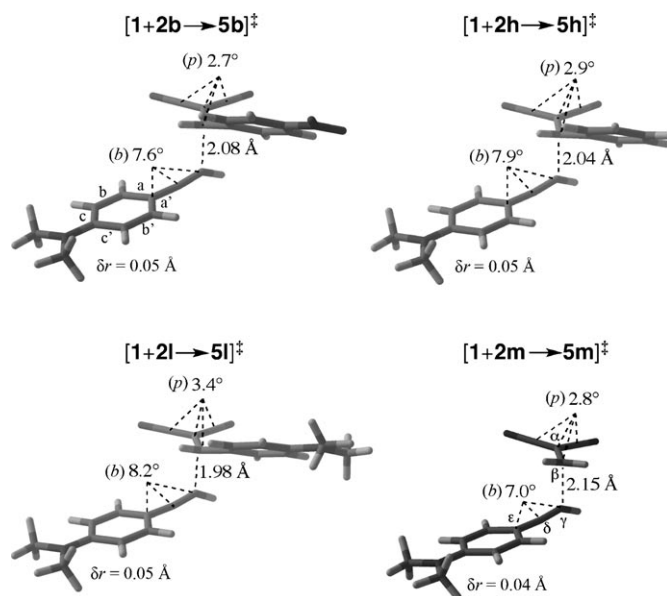


Figure 5. Optimized geometries (B3LYP/6-31G(d) with PCM solvation in acetonitrile) of TSs [1+2→5]<sup>‡</sup> for the reaction of **1** with **2m**, **2b**, **2h**, and **2l**. Relevant structural parameters are given. Bond angles (*b*) and pyramidalization (improper dihedral) angles (*p*) are in °, and bond lengths in Å; the quinoid character is defined as  $\delta r = [(a + a')/2 + (c + c')/2 - (b + b')]/2$ .

Pyramidalization (defined as the improper dihedral including both carbons of the two nitriles and the  $\alpha$  and  $\beta$  carbons) about the methyldine ( $\alpha$ ) carbon of the acceptor portion is significant and decreases in the direction of lowering activation energy as the TS becomes earlier ([1+2b→5b]<sup>‡</sup> (2.7°) < [1+2h→5h]<sup>‡</sup> (2.9°) < [1+2l→5l]<sup>‡</sup> (3.4°)). This pyramidalization is intermediate for the case of the reaction with 1,1-dicyanoethylene ([1+2m→5m]<sup>‡</sup> (2.8°)). For the donor portion, a substantial quinoid character<sup>[12]</sup> of the DMA group in the TSs ( $\delta r = 0.05$  Å for [1+2b→5b]<sup>‡</sup>, [1+2h→5h]<sup>‡</sup>, and [1+2l→5l]<sup>‡</sup>; see the caption of Figure 5 for definition), referenced to the structure of isolated **1** ( $\delta r = 0.03$  Å) at this level of theory, suggests that the donation from the amino substituent of the DMA residue is prominent. The quinoid character is slightly less when 1,1-dicyanoethylene is the electrophile ([1+2m→5m]<sup>‡</sup>;  $\delta r = 0.04$  Å). Additionally, deviation in the linearity of the  $\gamma$ - $\delta$ - $\epsilon$  bond angles of ~8° places a considerable cationic character at the central  $\delta$  carbon atom. This bond angle becomes linear for **5m**, **5b**, **5h**, and **5l** (see the Supporting Information for Cartesian coordinates) where the charge becomes further delo-

calized through the  $\pi$ -system in the zwitterionic ground-state. Finally, the forming bond between the  $\beta$  and  $\gamma$  positions varies considerably ([1+2m→5m]<sup>‡</sup> (2.15 Å) > [1+2b→5b]<sup>‡</sup> (2.08 Å) > [1+2h→5h]<sup>‡</sup> (2.04 Å) > [1+2l→5l]<sup>‡</sup> (1.98 Å)), again as a function of the accepting power of X. The TS [1+2m→5m]<sup>‡</sup> has the earliest (longest distance) structure of all.

Comparing the bond lengths of the computed cyclobutene moiety provides further insight into their tendency of ring-opening. The bond lengths between  $\beta$ - $\gamma$ ,  $\gamma$ - $\delta$  and  $\delta$ - $\alpha$  of all these cyclobutenes (**4b**, **4h**, **4l**, and **4m**) are similar; however, the length of the  $\alpha$ - $\beta$  bond varies about 0.05 Å throughout the series (for Cartesian coordinates and the pictorial illustration, see the Supporting Information). It is observed that the longer the  $\alpha$ - $\beta$  bond length, the smaller the barrier to ring-opening. Comparing **4b**, **4h**, and **4l**, we find a longer  $\alpha$ - $\beta$  bond length (1.65 Å) with the NMe<sub>2</sub> substituent, a shorter length with the NO<sub>2</sub> substituents (1.63 Å), and an intermediate value for the phenyl substituted cyclobutene (1.64 Å). This relatively small structural effect is presumably inductive in nature as the influencing substituent is separated by the sp<sup>3</sup>-hybridized  $\beta$ -carbon atom. Nonetheless the substituent effect, which may be acting on a partially diradical or zwitterionic electronic structure of the cyclobutene is sufficient to vary the cyclobutene energies in a range of about 9 kcal mol<sup>-1</sup>. Without any substituent (**4m**), this bond length is considerably shorter (1.60 Å). Given that electronic effects on the cyclobutene are attenuated by poor communication over the  $\beta$ -position, it is reasonable to assume that this effect is predominantly steric in nature. In the case of **4m**, the tight binding between the  $\alpha$  and  $\beta$  positions caused by a lack of destabilizing phenyl substitution leads to an additional 9 kcal mol<sup>-1</sup> (compare **4h** to **4m**) stabilization allowing the isolation of the cyclobutene as a stable intermediate, as discussed in the following section.

**Intermediate identification:** Comparing the computational free energy profile in our previous report for the reaction of **2m** with the results shown in the previous sections for **2b**, **2h**, and **2l**, it is interesting to notice that the higher-barrier process changed from the ring-opening step to the ring-formation step upon phenyl substitution. Since the cyclobutene intermediate was not found in any of the cases involving phenyl-substituted compounds, which have the RDS in the addition step, this change in relative barrier-height suggested the possibility of isolating the cyclobutene using **2m** as the electrophile.

To verify this postulate, **1** was mixed with **2m**, which was generated in situ from malononitrile and aqueous formaldehyde in DMF solution at 50 °C overnight. A yellow solid was isolated after column chromatography in 76% yield, and is stable at ambient condition for weeks without decomposition. The peak at *m/z* 223 in the mass spectrum indicated a molecular formula of C<sub>14</sub>H<sub>13</sub>N<sub>5</sub><sup>+</sup>, corresponding to the 1:1 adduct between **1** and **2m**. The very weak IR absorption of C≡N stretching at 2246 cm<sup>-1</sup> suggests a non-conjugated cyano functional group. In the <sup>1</sup>H NMR spectrum (CDCl<sub>3</sub>,

298 K), the aliphatic doublet signal at 3.3 ppm (2H,  $J=1.4$  Hz) together with the olefinic triplet signal at 6.2 ppm (1H,  $J=1.4$  Hz) immediately rule out the butadiene structure, but, to our delight, point to a cyclobutene **4m** which was further confirmed by X-ray analysis (Figure 6a).

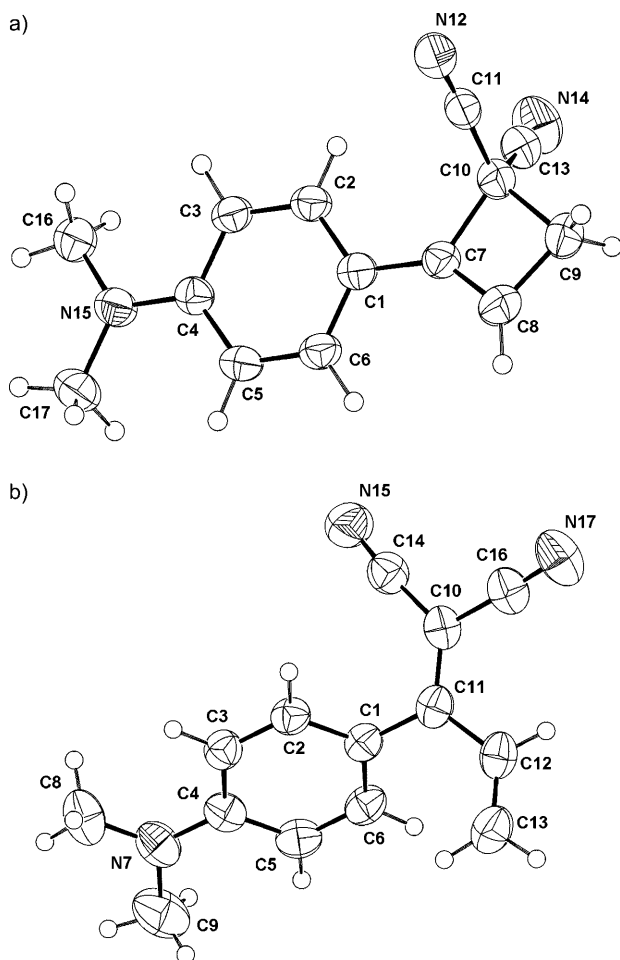


Figure 6. ORTEP plots of a) **4m** (223 K) and b) **3m** (223 K) with thermal ellipsoids shown at the 50% probability level. Selected bond lengths [Å], bond angles [°] and torsion angles [°]: **4m**: C1–C6 1.392(3), C1–C2 1.395(3), C2–C3 1.384(3), C3–C4 1.412(3), C4–C5 1.410(3), C5–C6 1.381(3), C7–C8 1.329(4), C7–C10 1.544(3), C8–C9 1.501(4), C9–C10 1.586(3); C11–C10–C13 109.2(2), C10–C7–C8–C9  $-0.3(2)$ , C2–C1–C7–C10  $-6.7(3)$ ; **3m**: C1–C2 1.396(3), C1–C6 1.401(3), C2–C3 1.374(3), C3–C4 1.410(3), C4–C5 1.408(3), C5–C6 1.373(3); C14–C10–C16 112.44(18), C2–C1–C11–C10  $-45.2(3)$ , C10–C11–C12–C13 162.5(2).

This cyclobutene molecule was further transformed into the 1,1-dicyanobuta-1,3-diene **3m** upon heating. In the real-time  $^1\text{H}$  NMR experiment in  $(\text{CDCl}_3)_2$  at 373 K, the two signals at 3.33 (d,  $J=0.9$  Hz) and 6.23 (t,  $J=0.9$  Hz) ppm of cyclobutene protons gradually vanished and three new sets of signals from terminal vinylic proton systems at 5.83 (dd,  $J=16.9, 0.8$  Hz), 6.06 (dd,  $J=10.6, 0.8$  Hz), and 7.08 (dd,  $J=16.9, 10.6$  Hz) ppm appeared (see the Supporting Information). The X-ray-quality crystal of the butadiene was obtained by the diffusion method and shows the *s-trans* geomet-

ry with non-planarity between the *N,N*-dimethylanilino and the dicyanovinyl moieties as observed in other phenyl-substituted analogues (Figure 6b).<sup>[5]</sup> The transformation is clean and quantitative, without involving any other intermediate (at least on the NMR time-scale), and its kinetics fits well into a first-order reaction (see the Supporting Information). Thus, this dicyanocyclobutene was, for the first time, isolated and identified as the true intermediate of the formal [2+2] cycloaddition between electron-rich acetylene and cyanoolefins, giving cyanobuta-1,3-dienes as the final products.

A closer look at the solid-state molecular structure of **4m** provides deeper information on the cyclobutene properties. The DMA and the cyclobutene rings arrange almost in the same plane with a small twist of  $6.68^\circ$ , making the whole molecule quasi- $C_s$  symmetric. The double bond length between C7–C8 is 1.329(4) Å, while the single bond lengths between C8–C9, C7–C10, and C9–C10 are 1.501(4), 1.544(3), and 1.586(3) Å, respectively. These bond lengths are all in the range of known bond length of cyclobutenes,<sup>[13]</sup> and the observed molecular geometry highly resembles that obtained from DFT calculations. However, it is noteworthy that the C7–C10 bond is significantly longer than the C8–C9 bond, and also than the typical  $C_{\text{sp}^3}\text{--}C_{\text{sp}^2}$  bond length in cyclobutenes.<sup>[13]</sup> It is known that, in phenyl-substituted cyclobutene, the substituted  $C_{\text{sp}^3}\text{--}C_{\text{sp}^2}$  bond is usually longer than the other unsubstituted one due to steric reasons,<sup>[14]</sup> making the corresponding bond angle C8–C7–C10  $93.2(2)^\circ$  smaller than C7–C8–C9  $96.5(2)^\circ$ , as a consequence of the geometrical constraint of the planar cyclobutene structure (sum of the four bond angles in the ring =  $360^\circ$ ).

## Conclusions

We have studied the reaction mechanism of the formal [2+2] cycloaddition–cycloreversion reaction between 4-(*N,N*-dimethylanilino)phenylacetylene (**1**) and a series of phenyl-substituted 1,1-dicyanovinyl derivatives **2b–2i** by means of UV/Vis and NMR spectroscopies and DFT calculations. From the experimental data, the reaction is clearly a quantitative transformation without by-product formation. The bimolecular, second-order kinetics shows a good linear free energy relationship with respect to the electronic effects of the dicyanovinyl electrophiles, indicating a strong zwitterionic character in the rate-determining step, which is most probably due to a transition state where the negative charge is located at the *gem*-dicyano-substituted homobenzylic position ( $\alpha$ -carbon) arising from nucleophilic attack of **1** onto the  $\beta$ -carbon of the dicyanovinyl moiety to form **5** according to the computed structures. For electrophiles **2b–2i**, the activation free energies range around  $22\text{--}27$  kcal mol $^{-1}$ , with negative activation entropy contributions of about  $-30$  cal K $^{-1}$  mol $^{-1}$  in DMF, on the order of those expected for a bimolecular reaction. The cyclobutenyl molecule **4m** generated from the cycloaddition between **1** and **2m** was isolated as the true reaction intermediate and transformed into the ring-opening dicyanobuta-1,3-diene **3m** upon heat-

ing. The small activation entropy ( $-11.4 \text{ cal K}^{-1} \text{ mol}^{-1}$ ) of ring-opening indicates a unimolecular RDS.

Four reaction sub-steps were identified on the computational reaction free energy profiles, where the addition step and the ring-opening processes were shown to have more importance to the overall reaction kinetics. The energy barriers for the addition step process for **2b**, **2h**, and **2i** are rate-determining as they are much higher in energy than those of their subsequent steps. The finding of a high barrier in the early stage of the bimolecular, multi-step reaction is also in accordance with the fact that the reactions follow simple second-order kinetics. Removing the phenyl substituent from the DCV group, however, changes the high-barrier step to the ring-opening process. As in the addition step, where the linear free energy relationship was found experimentally, there is also a substantial substituent effect on the ring-opening process. The barriers of this process were found to correlate with the ability of the substituent to affect the stability of the cyclobutene intermediates. The barrier heights calculated here were found to have a good quantitative agreement with the experimental values, suggesting the credibility of the proposed reaction mechanism.

While the mechanism for benzylidenemalononitriles has been treated in detail here, it would be too tenuous a generalization to assign the exact present mechanism to those reactions involving tricyanoethylene (TCE), TCNE, or TCNQ as the electrophiles nor do we offer a holistic mechanism for reactions involving metal acetylides as the nucleophiles. Our current finding suggests a reaction subclass that is highly sensitive to substitution with a roving rate-determining step. Additionally, a pre-equilibrium of the charge-transfer complexes for TCNE and TCNQ may be important. Preliminary kinetic experiments (unpublished results) for the reaction of **1** and TCNE (**2a**) offer an unclear picture as to whether the reaction is first or second order as both kinetic models give reasonable activation energies. It is reasonable that the addition step in this case would be considerably lower in energy than for the benzylidenemalononitriles and the ring-opening step much larger since the dicyanomethylidenes flank both the forming positively and negatively charged positions as the ring opens. Thus, either addition or ring-opening or both could be rate-determining in this case. Detailed mechanistic studies involving these electrophiles are ongoing to further elaborate the exciting complexity and sensitivity of this reaction subclass. As it stands, reactions involving electron-rich acetylenes and electron-poor cyanoolefins should proceed through a stepwise process involving zwitterionic and cyclobutenyl intermediates regardless of which TS is rate-determining.

## Experimental Section

**Materials and general methods:** Reagents were purchased at reagent grade from Acros, Sigma–Aldrich, and Fluka and used as received. Anhydrous  $\text{CH}_2\text{Cl}_2$  was freshly distilled from  $\text{CaH}_2$  under  $\text{N}_2$  atmosphere. Column chromatography was carried out with  $\text{SiO}_2$  60 (particle size

0.040–0.063 mm, 230–400 mesh; Fluka) and technical solvents. Thin-layer chromatography (TLC) was conducted on aluminum sheets or glass plate coated with  $\text{SiO}_2$  60  $\text{F}_{254}$  obtained from Merck; visualization with a UV lamp (254 or 366 nm). Melting points (M.p.) were measured on a Büchi B-540 melting-point apparatus in open capillaries and are uncorrected.  $^1\text{H}$  NMR and  $^{13}\text{C}$  NMR spectra were measured on a Bruker AV 400 instrument at  $20^\circ\text{C}$ . Chemical shifts are reported in ppm relative to the signal of tetramethylsilane. Residual solvent signals in the  $^1\text{H}$  and  $^{13}\text{C}$  NMR spectra were used as an internal reference. Coupling constants ( $J$ ) are given in Hz. The apparent resonance multiplicity is described as s (singlet), d (doublet), and dd (doublet of doublet). Infrared spectra (IR) were recorded on a Perkin–Elmer Spectrum BX instrument. UV/Vis spectra were recorded on a Varian Cary-500 spectrophotometer in a quartz cuvette (1 cm). The absorption wavelengths are reported in nm with the extinction coefficient  $\epsilon$  ( $\text{M}^{-1} \text{cm}^{-1}$ ) in parenthesis; shoulders are indicated as sh. High-resolution HR-EI-MS spectra were measured on a Hitachi-Perkin–Elmer VG-Tribrid spectrometer. The signal of the molecular ion ( $M^+$ ) is reported in  $m/z$  units. Compounds **3b**, **3e**, **3f**, **3g**, **3h**, **3k**, and **3l** and their corresponding dicyanovinyl precursor molecules **2b**, **2e**, **2f**, **2g**, **2h**, **2k**, and **2l** were prepared according to literature procedures<sup>[5]</sup> as were additional precursor molecules **2c**,<sup>[15a]</sup> **2d**,<sup>[15b]</sup> **2i**<sup>[15c]</sup> and **2j**,<sup>[15d]</sup> their NMR data and melting points are in accord with the literature values. New charge-transfer chromophores **3c**, **3d**, **3i**, and **3j** were prepared by the *General Method* (see below). Compound **3m** was prepared through in situ generation of precursor electrophile **2m** to yield first **4m**, as described below.

### UV/Vis measurements, initial-rate determination, and Eyring analysis:

The molar extinction coefficient and the initial-rate kinetics were measured with the Varian CARY 500 Scan UV-Vis-NIR Spectrophotometer, controlled by the CARY WinUV software in a Windows 2000 Professional operating system. The Scan application of CARY WinUV was used for molar extinction coefficient determination of a  $5 \times 10^{-5} \text{ M}$  solution in DMF at 298 K. For initial-rate measurement, the CARY Temperature Controller and Stir Control accessories were employed. The *Scanning Kinetics* application of CARY WinUV was used to control the appropriate temperature, the scan rate ( $600 \text{ nm min}^{-1}$ ), and scan range (550–400 nm), and to monitor the rate of product formation. The measured reactions were conducted in a 1 cm quartz cuvette charged with a stir-bar. For the cycloaddition reactions, **2b–2k** were added into the pre-heated DMF (3 mL) solution of **1** at 298, 323, 348, and 373 K. For the exceedingly slow reaction of **2l**, the temperatures were 353, 363, and 373 K. The concentration was  $5.05 \times 10^{-3} \text{ M}$  for each starting material. The spectra were collected for every 1 min (typically monitored over 20–40 min), and the product concentrations used for initial-rate calculation were converted from the recorded absorbances based on the corresponding extinction coefficients at room temperature. Each data point was collected three times, and the average value is presented herein with the standard deviation indicating the experimental error. All experimental rate constants are given in the Supporting Information.

From these variable temperature kinetic data, it was possible to perform Eyring analysis and extract the activation parameters  $\Delta H_{\text{exp}}^\ddagger$ ,  $\Delta S_{\text{exp}}^\ddagger$ , and  $\Delta G_{\text{exp}}^\ddagger$ . The initial rate of the unimolecular reaction of **4m** to **3m** was monitored at 333, 353, and 373 K by adding **4m** to the pre-heated neat DMF to obtain these parameters for the ring-opening step, using the same experimental conditions as for the other reactions. Fitting analyses of the Eyring plots are given in Supporting Information.

**Real-time NMR study of the reaction:** Real-time  $^1\text{H}$  NMR snapshots of the reaction were measured on a Bruker Avance DRX 500 spectrometer operating at 500.1 MHz for the  $^1\text{H}$  nucleus. The pulse angle was  $30^\circ$  and the acquisition time 5 s for each transient. The temperature was set by Bruker TopSpin, but the real temperature at the probehead region was measured externally with the Greisinger GMH 3710 high-precision thermometer connected to a platinum four-wire temperature sensor embedded in an NMR tube. A  $4.6 \times 10^{-2} \text{ M}$  solution of reactants in  $(\text{CD}_3)_2\text{SO}$  was freshly prepared and immediately charged into the pre-heated spectrometer for measurement. The temperature was assumed to reach equilibrium during the time of magnetic field adjustment. The spectra were

collected for every 20, 80, or 160 s, depending on the rapidness of individual reaction. Spectra procession was performed with MestReNova.

**X-ray analysis:** X-ray data collection was carried out on a Bruker Kap-paCCD diffractometer equipped with a graphite monochromator (Mo<sub>Kα</sub> radiation,  $\lambda = 0.71073 \text{ \AA}$ ) and an Oxford Cryostream low-temperature device. Cell dimensions were obtained by least-squares refinement of all measured reflections (HKL, Scapecap<sup>[16a]</sup>),  $\theta_{\max} = 27.5^\circ$ . All structures were solved by direct methods (SIR97<sup>[16b]</sup>). All non-hydrogen atoms were refined anisotropically, H-atoms isotropically by full matrix least-squares with SHELXL-97<sup>[16c]</sup> using experimental weights ( $1/[\sigma^2(I_o) + (I_o + I_c)^2/900]$ ).

**X-ray crystal structure of compound 4m:** Single crystals were obtained by slow diffusion of pentane into a solution of **4m** in CHCl<sub>3</sub> at  $-20^\circ\text{C}$ : C<sub>14</sub>H<sub>13</sub>N<sub>3</sub>,  $M_r = 223.28$ , crystal dimensions  $0.42 \times 0.2 \times 0.06 \text{ mm}$ , monoclinic space group  $P2_1/c$  (no. 14),  $\rho_{\text{calcd}} = 1.199 \text{ g cm}^{-3}$ ,  $Z = 4$ ,  $a = 6.7709(4)$ ,  $b = 7.6141(4)$ ,  $c = 24.105(2) \text{ \AA}$ ,  $\beta = 95.336(2)^\circ$ ,  $V = 1237.35(12) \text{ \AA}^3$  at 223(1) K. Number of measured and unique reflections 3716 and 2355, respectively ( $R_{\text{int}} = 0.043$ ). Final  $R(F) = 0.056$ ,  $wR(F^2) = 0.142$  for 206 parameters and 1467 reflections with  $I > 2\sigma(I)$  (corresponding  $R$ -values based on all 2355 reflections 0.102 and 0.174).<sup>[17]</sup>

**X-ray crystal structure of compound 3m:** Single crystals were obtained by slow diffusion of pentane into a solution of **3m** in CHCl<sub>3</sub> at  $-20^\circ\text{C}$ : C<sub>14</sub>H<sub>13</sub>N<sub>3</sub>,  $M_r = 223.28$ , crystal dimensions  $0.54 \times 0.3 \times 0.09 \text{ mm}$ , orthorhombic space group  $Pbca$  (no. 61),  $\rho_{\text{calcd}} = 1.173 \text{ g cm}^{-3}$ ,  $Z = 8$ ,  $a = 14.1701(6)$ ,  $b = 8.0015(3)$ ,  $c = 22.3043(8) \text{ \AA}$ ,  $V = 2528.9(2) \text{ \AA}^3$  at 223(1) K. Number of measured and unique reflections 5681 and 2879, respectively ( $R_{\text{int}} = 0.046$ ). Final  $R(F) = 0.081$ ,  $wR(F^2) = 0.186$  for 206 parameters and 1845 reflections with  $I > 2\sigma(I)$  (corresponding  $R$ -values based on all 879 reflections 0.118 and 0.208).<sup>[17]</sup>

**X-ray crystal structure of compound 3c:** Crystals were grown by slow diffusion of pentane into a solution of **3c** in CHCl<sub>3</sub> at room temperature in a sealed container. The ORTEP plot of **3c** can be found in Supporting Information: C<sub>21</sub>H<sub>19</sub>N<sub>3</sub>,  $M_r = 324.39$ , crystal dimensions  $0.36 \times 0.075 \times 0.025 \text{ mm}$ , monoclinic space group  $P2_1/c$  (no. 14),  $\rho_{\text{calcd}} = 1.192 \text{ g cm}^{-3}$ ,  $Z = 4$ ,  $a = 9.6650(4)$ ,  $b = 7.8764(6)$ ,  $c = 23.977(2) \text{ \AA}$ ,  $\beta = 97.899(5)^\circ$ ,  $V = 1808.0(2) \text{ \AA}^3$  at 170(1) K. Number of measured and unique reflections 8095 and 2433, respectively ( $R_{\text{int}} = 0.077$ ). Final  $R(F) = 0.055$ ,  $wR(F^2) = 0.141$  for 290 parameters and 1768 reflections with  $I > 2\sigma(I)$  (corresponding  $R$ -values based on all 2433 reflections 0.085 and 0.165).<sup>[17]</sup>

**General method for the synthesis of 3c, 3d, 3i, and 3j:** A solution of DCV derivative **2c**, **2d**, **2i**, or **2j** (100 mg) in acetonitrile (6 mL) and **1** (1 equiv) was stirred at reflux until complete conversion (determined by LC-MS). The solvent was removed first by rotary evaporation, then under higher vacuum to yield the crude product. The purification of each product is described below.

**{(2E)-3-(4-Cyanophenyl)-1-[4-(dimethylamino)phenyl]-2-propen-1-ylidene}malononitrile (3c):** Following the general method, **3c** was obtained (175 mg, 96%) after passing the crude material through a short plug of SiO<sub>2</sub> with CH<sub>2</sub>Cl<sub>2</sub> as eluent and collecting the red-colored band. M.p. 214–215 °C; <sup>1</sup>H NMR (CDCl<sub>3</sub>, 400 MHz):  $\delta = 3.10$  (s, 6H; NMe<sub>2</sub>), 6.76 (d,  $J = 9.0 \text{ Hz}$ , 2H; PhNMe<sub>2</sub>), 7.01 (d,  $J = 15.7 \text{ Hz}$ , 1H; CH=CH), 7.41 (d,  $J = 9.0 \text{ Hz}$ , 2H; PhNMe<sub>2</sub>), 7.56 (d,  $J = 15.7 \text{ Hz}$ , 1H; CH=CH), 7.62 (d,  $J = 8.4 \text{ Hz}$ , 2H; PhCN), 7.69 ppm (d,  $J = 8.4 \text{ Hz}$ , 2H; PhCN); <sup>13</sup>C NMR (CDCl<sub>3</sub>, 100 MHz):  $\delta = 40.03$ , 79.02, 111.42, 113.83, 113.91, 114.65, 118.18, 119.32, 128.54, 128.61, 131.71, 132.75, 138.86, 144.81, 152.99, 169.37 ppm; IR (neat):  $\tilde{\nu} = 3050$  (vw), 2986 (vw), 2938 (vw), 1717 (m), 1685 (m), 1265 (s), 1221 (m), 740 (vs), 631 cm<sup>-1</sup> (s); UV/Vis (DMF):  $\lambda_{\text{max}}$  ( $\epsilon$ ) = 345 (26400), 474 nm (9400 m<sup>-1</sup>cm<sup>-1</sup>); HR-EI-MS  $m/z$ : calcd for C<sub>21</sub>H<sub>16</sub>N<sub>4</sub><sup>+</sup>: 324.1369; found: 324.1369 ([M]<sup>+</sup>).

**Methyl 4-[(1E)-4,4-dicyano-3-[4-(dimethylamino)phenyl]buta-1,3-dien-1-yl]benzoate (3d):** Following the general method, **3d** was obtained (135 mg, 80%) after column chromatography (SiO<sub>2</sub>, hexane:CH<sub>2</sub>Cl<sub>2</sub> = 2:1) and collecting the red-colored band. M.p. 211–212 °C; <sup>1</sup>H NMR (CDCl<sub>3</sub>, 400 MHz):  $\delta = 3.10$  (s, 6H; NMe<sub>2</sub>), 3.94 (s, 3H; CO<sub>2</sub>Me), 6.76 (2,  $J = 8.7 \text{ Hz}$ , 2H; PhNMe<sub>2</sub>), 7.04 (d,  $J = 15.7 \text{ Hz}$ , 1H; CH=CH), 7.41 (d,  $J = 8.7 \text{ Hz}$ , 2H; PhNMe<sub>2</sub>), 7.67–7.53 (m, 3H; CH=CH, PhCO<sub>2</sub>Me), 8.06 ppm (d,  $J = 8.2 \text{ Hz}$ , 2H; PhCO<sub>2</sub>Me); <sup>13</sup>C NMR (CDCl<sub>3</sub>, 100 MHz):  $\delta = 40.05$ , 52.36, 78.49, 111.40, 114.06, 114.85, 119.60, 127.44, 128.25, 130.25, 131.71,

131.87, 138.81, 146.24, 152.90, 166.27, 170.03 ppm; IR (neat):  $\tilde{\nu} = 2951$  (vw), 2905 (vw), 2824 (vw), 2361 (w) 2343 (w), 2216 (m), 1720 (s), 1600 (vs), 1492 (s), 1283 cm<sup>-1</sup> (s); UV/Vis (DMF):  $\lambda_{\text{max}}$  ( $\epsilon$ ) = 352 (27100), 470 nm (9300 m<sup>-1</sup>cm<sup>-1</sup>); HR-EI-MS  $m/z$ : calcd for C<sub>22</sub>H<sub>14</sub>N<sub>3</sub>O<sub>2</sub><sup>+</sup>: 357.1472; found: 357.1473 ([M]<sup>+</sup>).

**{(2E)-3-Biphenyl-4-yl-1-[4-(dimethylamino)phenyl]prop-2-en-1-ylidene}malononitrile (3i):** Following the general method, **3i** was obtained (139 mg, 86%) after washing with Et<sub>2</sub>O. M.p. 200–202 °C; <sup>1</sup>H NMR (CDCl<sub>3</sub>, 400 MHz):  $\delta = 3.10$  (s, 6H; NMe<sub>2</sub>), 6.77 (d,  $J = 9.0 \text{ Hz}$ , 2H; PhNMe<sub>2</sub>), 7.07 (d,  $J = 15.6 \text{ Hz}$ , 1H; CH=CH), 7.48–7.36 (m, 5H, Ph), 7.56 (d,  $J = 15.6 \text{ Hz}$ , 1H; CH=CH), 7.65–7.60 ppm (m, 6H; Ph); <sup>13</sup>C NMR (CDCl<sub>3</sub>, 100 MHz):  $\delta = 40.06$ , 111.37, 114.33, 115.15, 119.96, 125.10, 127.06, 127.71, 128.12, 128.97, 129.07, 131.67, 133.74, 139.85, 143.86, 147.59, 152.77, 170.75 ppm (1 peak of C(CN)<sub>2</sub> is overlapped with the solvent peaks); IR (neat):  $\tilde{\nu} = 2923$  (vw), 2860 (vw), 2826 (vw), 2360 (vw), 2208 (s), 1594 (vs), 1481 (s), 1376 (s), 1347 (s), 1172 cm<sup>-1</sup> (s); UV/Vis (DMF):  $\lambda_{\text{max}}$  ( $\epsilon$ ) = 382 (31300), 454 nm (sh, 9900 m<sup>-1</sup>cm<sup>-1</sup>); HR-EI-MS  $m/z$ : calcd for C<sub>26</sub>H<sub>21</sub>N<sub>3</sub><sup>+</sup>: 375.1730; found: 375.1729 ([M]<sup>+</sup>).

**[(2E)-1-[4-(Dimethylamino)phenyl]-3-(4-methylphenyl)prop-2-en-1-ylidene]malononitrile (3j):** Following the general method, **3j** was obtained (150 mg, 81%) after washing with Et<sub>2</sub>O. M.p. 151–154 °C; <sup>1</sup>H NMR (CDCl<sub>3</sub>, 400 MHz):  $\delta = 2.39$  (s, 3H; PhMe), 3.09 (s, 6H; PhNMe<sub>2</sub>), 6.76 (d,  $J = 9.0 \text{ Hz}$ , 2H; PhNMe<sub>2</sub>), 7.00 (d,  $J = 15.6 \text{ Hz}$ , 1H; CH=CH), 7.21 (d,  $J = 8.2 \text{ Hz}$ , 2H; PhMe), 7.39 (d,  $J = 9.0 \text{ Hz}$ , 2H; PhMe); 7.44 (d,  $J = 8.2 \text{ Hz}$ , 2H; PhMe); 7.49 ppm (d,  $J = 15.6 \text{ Hz}$ , 1H; CH=CH); <sup>13</sup>C NMR (CDCl<sub>3</sub>, 100 MHz):  $\delta = 21.57$ , 40.03, 111.32, 114.36, 115.19, 120.03, 124.23, 128.57, 129.87, 131.61, 132.12, 141.89, 148.22, 152.70, 171.04 ppm (1 peak of C(CN)<sub>2</sub> is overlapped with the solvent peaks); IR (neat):  $\tilde{\nu} = 3055$  (vw), 2987 (vw), 2868 (vw), 2821 (vw), 2217 (m), 1600 (s), 1491 (m), 1371 (m), 1345 (m), 1265 (m), 1172 (m), 735 cm<sup>-1</sup> (s); UV/Vis (DMF):  $\lambda_{\text{max}}$  ( $\epsilon$ ) = 368 (22100), 460 nm (8300 m<sup>-1</sup>cm<sup>-1</sup>); HR-EI-MS  $m/z$ : calcd for C<sub>21</sub>H<sub>19</sub>N<sub>3</sub><sup>+</sup>: 313.1573; found: 313.1575 ([M]<sup>+</sup>).

**2-[4-(Dimethylamino)phenyl]cyclobut-2-ene-1,1-dicarbonitrile (4m):** Alkyne **1** (100 mg, 0.69 mmol) was added into a DMF (5 mL) solution of formaldehyde (36% solution in water, 63  $\mu\text{L}$ , 0.83 mmol) and malononitrile (45.5 mg, 0.69 mmol). The mixture was stirred at 50 °C for 18 h. DMF and water were removed under vacuum, and the residue was purified by column chromatography (SiO<sub>2</sub>, CH<sub>2</sub>Cl<sub>2</sub>/hexane 1:1 → 2:1) to give **4m** as a yellow solid (117 mg, 76%).  $R_f = 0.25$  (CH<sub>2</sub>Cl<sub>2</sub>/hexane = 2:1); m.p. > 133 °C (the molecule opened into the corresponding butadiene around 100 °C at a discernable rate; thus the m.p. could not be recorded); <sup>1</sup>H NMR (CDCl<sub>3</sub>, 300 MHz):  $\delta = 3.01$  (s, 6H; NMe<sub>2</sub>), 3.30 (d,  $J = 1.4 \text{ Hz}$ , 2H; CH<sub>2</sub> in cyclobutene), 6.19 (t,  $J = 1.4 \text{ Hz}$ , 1H; CH=C in cyclobutene), 6.71 (d,  $J = 8.9 \text{ Hz}$ , 2H; PhNMe<sub>2</sub>), 7.36 ppm (d,  $J = 8.9 \text{ Hz}$ , 1H; PhNMe<sub>2</sub>); <sup>13</sup>C NMR (CDCl<sub>3</sub>, 100 MHz):  $\delta = 29.63$ , 39.27 40.03, 111.88, 114.29, 116.65, 124.11, 125.76, 140.79, 151.27 ppm; IR (neat):  $\tilde{\nu} = 2245$  (vw), 1627 (m), 1603 (m), 1522 (m), 1364 cm<sup>-1</sup> (m); HR-EI-MS  $m/z$ : calcd for C<sub>14</sub>H<sub>13</sub>N<sub>3</sub><sup>+</sup>: 223.1109; found: 223.1102 ([M]<sup>+</sup>); elemental analysis (%) calcd for C<sub>14</sub>H<sub>13</sub>N<sub>3</sub>: C 75.31, H 5.87, N 18.82; found: C 75.25, H 5.83, N 18.66.

**[1-[4-(Dimethylamino)phenyl]prop-2-en-1-ylidene]malononitrile (3m):** A solution of **4m** (50 mg, 0.22 mmol) in 1,1,2,2-tetrachloroethane (5 mL) was stirred at 80 °C for 10 h. The solvent was removed under vacuum to provide the product as a red solid (50 mg, 100%).  $R_f = 0.17$  (CH<sub>2</sub>Cl<sub>2</sub>/hexane = 1:1); m.p. 115–116 °C; <sup>1</sup>H NMR (CDCl<sub>3</sub>, 400 MHz):  $\delta = 3.07$  (s, 6H; NMe<sub>2</sub>), 5.79 (dd,  $J = 16.9$ , 0.8 Hz, 1H; CH=CH<sub>2</sub>), 6.01 (dd,  $J = 10.6$ , 0.8 Hz, 1H; CH=CH<sub>2</sub>), 6.72 (d,  $J = 9.0 \text{ Hz}$ , 2H; PhNMe<sub>2</sub>), 7.10 (dd,  $J = 16.9$ , 10.6 Hz, 1H; CH=CH<sub>2</sub>), 7.41 ppm (d,  $J = 9.0 \text{ Hz}$ ; PhNMe<sub>2</sub>); <sup>13</sup>C NMR (CDCl<sub>3</sub>, 100 MHz):  $\delta = 39.94$ , 78.07, 111.19, 113.78, 114.71, 119.31, 131.86, 133.12, 134.22, 152.98, 170.43 ppm; IR (neat):  $\tilde{\nu} = 2218$  (m), 1600 (m), 1503 (m), 1372 cm<sup>-1</sup> (m); UV/Vis (DMF):  $\lambda_{\text{max}}$  ( $\epsilon$ ) = 436 nm (16800 m<sup>-1</sup>cm<sup>-1</sup>); HR-EI-MS  $m/z$ : calcd for C<sub>14</sub>H<sub>13</sub>N<sub>3</sub><sup>+</sup>: 223.1109; found: 223.1103.

## Acknowledgements

This work was supported by ETH Research Council. The authors thank Dr. Marc-Olivier Ebert (ETH) for the help in NMR experiments. We are grateful for access to the Competence Center for Computational Chemistry (C4) Obelix cluster (ETH). Y.-L. W. Acknowledges the receipt of Stipendienfonds der Schweizerischen Chemischen Industrie (SSCI).

- [1] a) J. M. Tour, *Chem. Rev.* **1996**, *96*, 537–553. b) Focus Issue on “Organic Electronics”: *J. Mater. Res.* **2004**, *19*, 1887–2203, edited by F. Faupel, C. Dimitrakopoulos, A. Kahn, C. Wöll. c) Special Issue on “Organic Electronics and Optoelectronics”: *Chem. Rev.* **2007**, *107*, 923–1386, edited by F. Faupel, C. Dimitrakopoulos, A. Kahn, C. Wöll.
- [2] H. C. Kolb, M. G. Finn, K. B. Sharpless, *Angew. Chem.* **2001**, *113*, 2056–2075; *Angew. Chem. Int. Ed.* **2001**, *40*, 2004–2021.
- [3] a) T. Michinobu, C. Boudon, J. P. Gisselbrecht, P. Seiler, B. Frank, N. N. P. Moonen, M. Gross, F. Diederich, *Chem. Eur. J.* **2006**, *12*, 1889–1905; b) M. Kivala, C. Boudon, J.-P. Gisselbrecht, P. Seiler, M. Gross, F. Diederich, *Chem. Commun.* **2007**, 4731–4733; c) P. Reutenauer, M. Kivala, P. D. Jarowski, C. Boudon, J.-P. Gisselbrecht, M. Gross, F. Diederich, *Chem. Commun.* **2007**, 4898–4900; d) M. Kivala, C. Boudon, J.-P. Gisselbrecht, B. Enko, P. Seiler, I. B. Müller, N. Langer, P. D. Jarowski, G. Gescheidt, F. Diederich, *Chem. Eur. J.* **2009**, *15*, 4111–4123; e) S.-i. Kato, M. Kivala, W. B. Schweizer, C. Boudon, J.-P. Gisselbrecht, F. Diederich, *Chem. Eur. J.* **2009**, *15*, 8687–8691.
- [4] a) B. Esembeson, M. L. Scimeca, T. Michinobu, F. Diederich, I. Biaggio, *Adv. Mater.* **2008**, *20*, 4584–4587; b) C. Koos, P. Vorreau, T. Vallaitis, P. Dumon, W. Bogaerts, R. Baets, B. Esembeson, I. Biaggio, T. Michinobu, F. Diederich, W. Freude, J. Leuthold, *Nat. Photonics* **2009**, *3*, 216–219.
- [5] P. D. Jarowski, Y.-L. Wu, C. Boudon, J.-P. Gisselbrecht, M. Gross, W. B. Schweizer, F. Diederich, *Org. Biomol. Chem.* **2009**, *7*, 1312–1322.
- [6] S. T. Diver, A. J. Giessert, *Chem. Rev.* **2004**, *104*, 1317–1382.
- [7] a) R. Gompper, *Angew. Chem.* **1969**, *81*, 348–363; *Angew. Chem. Int. Ed. Engl.* **1969**, *8*, 312–327; b) R. Huisgen, *Acc. Chem. Res.* **1977**, *10*, 117–124; c) R. Huisgen, *Acc. Chem. Res.* **1977**, *10*, 199–206; d) A. J. Fatiadi, *Synthesis* **1987**, 749–789; e) K. Inanaga, K. Takasu, M. Ihara, *J. Am. Chem. Soc.* **2005**, *127*, 3668–3669; f) R. W. M. Aben, J. Goudriaan, J. M. M. Smits, H. W. Scheeren, *Synthesis* **1993**, 37–39; g) H. K. Hall, Jr. M. Abdelkader, M. E. Glogowski, *J. Org. Chem.* **1982**, *47*, 3691–3694; h) K. C. Brannock, A. Bell, R. D. Burpitt, C. A. Kelly, *J. Org. Chem.* **1964**, *29*, 801–812; i) I. Nakamura, R. Nagata, T. Nemoto, M. Terada, Y. Yamamoto, T. Späth, A. de Meijere, *Eur. J. Org. Chem.* **2007**, 4479–4482.
- [8] The acetylides of transition metals are known to undergo thermal [2+2] cycloaddition; however, their d orbital participation makes concerted process possible. For example of the reaction of TCNE, see: a) M. I. Bruce, J. R. Rodgers, M. R. Snow, A. G. Swincer, *J. Chem. Soc. Chem. Commun.* **1981**, 271–271; b) M. I. Bruce, T. W. Hambley, J. R. Rodgers, M. R. Snow, A. G. Swincer, *J. Organomet. Chem.* **1982**, *226*, C1–C4; c) M. I. Bruce, T. W. Hambley, M. R. Snow, A. G. Swincer, *Organometallics* **1985**, *4*, 494–500; d) M. I. Bruce, M. J. Liddell, M. R. Snow, E. R. T. Tiekink, *Organometallics* **1988**, *7*, 343–350; e) M. I. Bruce, T. W. Hambley, M. J. Liddell, A. G. Swincer, E. R. T. Tiekink, *Organometallics* **1990**, *9*, 2886–2898; f) M. I. Bruce, M. E. Smith, B. W. Skelton, A. H. White, *J. Organomet. Chem.* **2001**, *637–639*, 484–499. For TCNQ, see: g) K.-i. Onuma, Y. Kai, N. Yasuoka, N. Kasai, *Bull. Chem. Soc. Jpn.* **1975**, *48*, 1696–1700. For dicyanovinyls, see: h) M. I. Bruce, P. A. Humphrey, M. R. Snow, E. R. T. Tiekink, *J. Organomet. Chem.* **1986**, *303*, 417–427; i) C.-W. Chang, Y.-C. Lin, G.-H. Lee, Y. Wang, *J. Chem. Soc. Dalton Trans.* **1999**, 4223–4230.
- [9] a) J. Ø. Madsen, S.-O. Lawesson, *Tetrahedron* **1974**, *30*, 3481–3492; b) J. Ficini, *Tetrahedron* **1976**, *32*, 1449–1486; c) H. C. Brown, G. G. Pai, *J. Org. Chem.* **1982**, *47*, 1608–1610; d) M. L. M. Pennings, D. N. Reinhoudt, *J. Org. Chem.* **1982**, *47*, 1816–1823; e) G. Himbert, W. Brunn, *Chem. Ber.* **1984**, *117*, 642–653; f) G. Himbert, W. Brunn, *Liebigs Ann. Chem.* **1985**, 2206–2216; g) G. Himbert, S. Kosack, *Chem. Ber.* **1988**, *121*, 2053–2057.
- [10] C. Hansch, A. Leo, R. W. Taft, *Chem. Rev.* **1991**, *91*, 165–195.
- [11] Gaussian 03, Revision C.02, M. J. Frisch, G. W. Trucks, H. B. Schlegel, G. E. Scuseria, M. A. Robb, J. R. Cheeseman, J. Montgomery, Jr., T. Vreven, K. N. Kudin, J. C. Burant, J. M. Millam, S. S. Iyengar, J. Tomasi, V. Barone, B. Mennucci, M. Cossi, G. Scalmani, N. Rega, G. A. Petersson, H. Nakatsuji, M. Hada, M. Ehara, K. Toyota, R. Fukuda, J. Hasegawa, M. Ishida, T. Nakajima, Y. Honda, O. Kitao, H. Nakai, M. Klene, X. Li, J. E. Knox, H. P. Hratchian, J. B. Cross, C. Adamo, V. Bakken, C. Adamo, J. Jaramillo, R. Gomperts, R. E. Stratmann, O. Yazyev, A. J. Austin, R. Cammi, C. Pomelli, J. W. Ochterski, P. Y. Ayala, K. Morokuma, G. A. Voth, P. Salvador, J. J. Dannenberg, V. G. Zakrzewski, S. Dapprich, A. D. Daniels, M. C. Strain, O. Farkas, D. K. Malick, A. D. Rabuck, K. Raghavachari, J. B. Foresman, J. V. Ortiz, Q. Cui, A. G. Baboul, S. Clifford, J. Cioslowski, B. B. Stefanov, G. Liu, A. Liashenko, P. Piskorz, I. Komaromi, R. L. Martin, D. J. Fox, T. Keith, M. A. Al-Laham, C. Y. Peng, A. Nanayakkara, M. Challacombe, P. M. W. Gill, B. Johnson, W. Chen, M. W. Wong, C. Gonzalez, J. A. Pople, Gaussian, Inc., Wallingford CT, **2004**.
- [12] C. Dehu, F. Meyers, J. L. Brédas, *J. Am. Chem. Soc.* **1993**, *115*, 6198–6206.
- [13] a) F. H. Allen, *Acta Crystallogr. Sect. B* **1984**, *40*, 64–72; b) F. H. Allen, O. Kennard, D. G. Watson, L. Brammer, A. G. Orpen, R. Taylor, *J. Chem. Soc. Perkin Trans. 2* **1987**, S1–S19.
- [14] Similar bond length relationships were found in 38 out of 39 asymmetric 1-phenylcyclobutenes according to Cambridge Structural Database analysis (CSD Version 5.30 + 4 updates, Sep. 2009). For example: A. Usman, I. A. Razak, H.-K. Fun, S. Chantrapromma, B.-G. Zhao, J.-H. Xu, *Acta Crystallogr. Sect. E* **2001**, *57*, o990–o991.
- [15] a) L. Horner, K. Klüpfel, *Liebigs Ann. Chem.* **1955**, *591*, 69–98; b) T. B. Posner, C. D. Hall, *J. Chem. Soc. Perkin Trans. 2* **1976**, 729–732; c) M. Mantri, O. de Graaf, J. van Veldhoven, A. Göblyös, J. K. von F. D. Künzel, T. Mulder-Krieger, R. Link, H. de Vries, M. W. Beukers, J. Brussee, A. P. Ijzerman, *J. Med. Chem.* **2008**, *51*, 4449–4455; d) M. M. Heravi, M. H. Tehrani, K. Bakhtiari, H. A. Oskooie, *J. Chem. Res.* **2006**, 561–562.
- [16] a) Z. Otwinowski, W. Minor, *Methods Enzymol.* **1997**, *276*, 307–326; b) A. Altomare, M. C. Burla, M. Camalli, G. L. Cascarano, C. Giacovazzo, A. Guagliardi, A. G. G. Moliterni, G. Polidori, R. Spagna, *J. Appl. Crystallogr.* **1999**, *32*, 115; c) SHELXL97, Program for the Refinement of Crystal Structures, G. M. Sheldrick, University of Göttingen, Göttingen, **1997**.
- [17] CCDC-744043 (**4m**), CCDC-744044 (**3m**), and CCDC-748317 (**3c**), contains the supplementary crystallographic data for this paper. These data can be obtained free of charge from The Cambridge Crystallographic Data Centre via [www.ccdc.cam.ac.uk/data\\_request/cif](http://www.ccdc.cam.ac.uk/data_request/cif).

Received: September 25, 2009  
Published online: December 9, 2009